

Research Articles: Systems/Circuits

Fast-spiking interneurons of the premotor cortex contribute to initiation and execution of spontaneous actions

https://doi.org/10.1523/JNEUROSCI.0750-22.2023

Cite as: J. Neurosci 2023; 10.1523/JNEUROSCI.0750-22.2023

Received: 11 April 2022 Revised: 24 March 2023 Accepted: 28 March 2023

This Early Release article has been peer-reviewed and accepted, but has not been through the composition and copyediting processes. The final version may differ slightly in style or formatting and will contain links to any extended data.

Alerts: Sign up at www.jneurosci.org/alerts to receive customized email alerts when the fully formatted version of this article is published.

Copyright © 2023 Giordano et al.

This is an open-access article distributed under the terms of the Creative Commons Attribution 4.0 International license, which permits unrestricted use, distribution and reproduction in any medium provided that the original work is properly attributed.

Fast-spiking interneurons of the premotor cortex contribute to

initiation and execution of spontaneous actions

- 3 Abbreviated title: Fs interneurons contribute to action initiation
 - Nadia Giordano^{1,2,8}, Claudia Alia^{1,8*}, Lorenzo Fruzzetti^{1,3,4}, Maria Pasquini^{3,4}, Giulia Palla^{1,2}, Alberto Mazzoni^{3,4}, Silvestro Micera^{3,4,5}, Leonardo Fogassi⁶, Luca Bonini⁶, Matteo Caleo^{7,1}
- ⁶ ¹Neuroscience Institute, National Research Council (CNR), v. G. Moruzzi 1, 56124 PI, Italy.
- ⁷ ²Scuola Normale Superiore, P.zza dei Cavalieri 7, 56127 PI, Italy.
- ³The BioRobotics Institute, Scuola Superiore Sant'Anna, v. le Rinaldo Piaggio 34, 56025,
 Pontedera, PI, Italy.
- ⁴Department of Excellence in Robotics & IA, Scuola Superiore Sant'Anna, PI, Italy.
- ¹¹ ⁵Bertarelli Foundation Chair in Translational NeuroEngineering Laboratory, École Polytechnique
- 12 Fédérale de Lausanne (EPFL), Centre for Neuroprosthetics and Institute of Bioengineering,
- 13 Lausanne, Switzerland.

1

2

4 5

- ⁶Department of Medicine and Surgery, University of Parma, v. Volturno 39/E, 43125 PR, Italy.
- ¹⁵ ⁷Department of Biomedical Sciences, University of Padua, via G. Colombo 3, 35121 Padua, Italy.
- ¹⁶ ⁸These authors contributed equally.
- 17 * Correspondence: <u>alia@in.cnr.it</u>
- 18 Number of pages: 39
- 19 Number of figures: 11 Figures
- 20 Number of tables: 2 Tables
- 21 Number of words for abstract: 169
- 22 Number of words for introduction: 439
- 23 Number of words for discussion: 1224
- 24 Conflict of interest statement: The authors declare no competing financial interests.

Dedications: This manuscript is dedicated to the memory of Prof. Matteo Caleo (DOD 04.12.2022), who was a model for enthusiasm and dedication in science and who introduced us (N. G. and C. A.) to the extraordinary world of this story.

Acknowledgments: We thank Francesca Biondi (CNR PI) for excellent animal care. This project has received funding from: H2020 EXCELLENT SCIENCE-European Research Council (ERC) under grant agreement 692943 (BrainBIT); Regione Toscana (PERSONA project, bando Salute 2018); Fondazione Cassa di Risparmio di Padova e Rovigo (Foundation Cariparo, project #52000 to M.C.); Ministry of University (MUR) grant FARE2020, project n. R20NJ7BBA7 "CIRCEM" to L.B.

34 Abstract

35 Planning and execution of voluntary movement depend on the contribution of distinct classes of neurons in primary motor and premotor areas. However, timing and pattern of activation of 36 GABAergic cells during specific motor behaviors remain only partly understood. Here, we directly 37 38 compared the response properties of putative pyramidal neurons (PNs) and GABAergic fast-39 spiking neurons (FSNs) during spontaneous licking and forelimb movements in male mice. 40 Recordings centered on the face/mouth motor field of the anterolateral motor cortex revealed that FSNs fire longer than PNs and earlier for licking, but not for forelimb movements. Computational 41 analysis revealed that FSNs carry vastly more information than PNs about the onset of 42 43 movement. While PNs differently modulate their discharge during distinct motor acts, most FSNs respond with a stereotyped increase in firing rate. Accordingly, the informational redundancy was 44 greater among FSNs than PNs. Finally, optogenetic silencing of a subset of FSNs reduced 45 spontaneous licking movement. These data suggest that a global rise of inhibition contributes to 46 the initiation and execution of spontaneous motor actions. 47

48

49 Significance Statement

Our study contributes to clarifying the causal role of fast-spiking neurons (FSNs) in driving 50 51 initiation and execution of specific, spontaneous movements. Within the face/mouth motor field of 52 mice premotor cortex, FSNs fire before pyramidal neurons (PNs) with a specific activation 53 pattern: they reach their peak of activity earlier than PNs during the initiation of licking, but not of 54 forelimb, movements; duration of FSNs activity is also greater and exhibits less selectivity for the movement type, as compared to that of PNs. Accordingly, FSNs appear to carry more redundant 55 information than PNs. Optogenetic silencing of FSNs reduced spontaneous licking movement, 56 suggesting that FSNs contribute to the initiation and execution of specific spontaneous 57 movements, possibly by sculpting response selectivity of nearby PNs. 58

59 Introduction

60 Activity occurring before the initiation of voluntary movements is critical for action planning and execution (Churchland, 2006; Gao et al., 2018; Godschalk et al., 1985; Guo et al., 2014; Li et al., 61 2016; Murakami et al., 2014; Weinrich and Wise, 1982; Wise and Mauritz, 1985). Specifically, 62 63 premotor areas act as a conductor to orchestrate the network activity of the rest of the motor 64 modules, on a moment-by-moment basis, and exhibit tuning for specific movements (Churchland, 2006; Churchland and Shenoy, 2007; Georgopoulos et al., 1982; Godschalk et al., 1985; 65 Hocherman and Wise, 1991; Messier and Kalaska, 2000; Riehle and Requin, 1993). How do 66 distinct neuronal classes contribute to this process? The anticipatory activity of pyramidal 67 neurons (PNs) has been previously examined (Svoboda and Li, 2018), however little is known on 68 69 the contribution of GABAergic cells to these cortical computations (Isomura et al., 2009; Kaufman et al., 2013; Merchant et al., 2008). 70

71 Fast-spiking neurons (FSNs) are the most prevalent type of GABAergic interneurons in the cortex (Lourenço et al., 2020a) and are well suited to shape neuronal dynamics (Isomura et al., 2009; 72 Merchant et al., 2008; Pi et al., 2013; Polack et al., 2013; Sachidhanandam et al., 2016). FSNs 73 exhibit narrow action potentials and high spontaneous discharge rates (Merchant et al., 2012; 74 75 Swanson and Maffei, 2019). In the rodent sensory cortex, FSNs contribute to sharpening the tuning of cortical neurons to preferred stimuli (Isaacson and Scanziani, 2011; Liu et al., 2011, p. 76 20122; Poo and Isaacson, 2009; Tan et al., 2011; Wu et al., 2008). In mice primary motor cortex, 77 78 they fire before PNs during reaching movements (Estebanez et al., 2017), supporting a dynamic role of inhibition in shaping the tuning of PNs while routing information to the subsequent motor 79 module (Merchant et al., 2008). 80

Here, we recorded premotor neuronal activity from the anterior-lateral motor cortex (ALM, Chen et al., 2017; Guo et al., 2014; Komiyama et al., 2010), which partially overlaps with the rostral forelimb area (RFA Tennant et al., 2011; Vallone et al., 2016), in head-restrained mice allowed to either spontaneously lick or pull a handle in a robotic device (Spalletti et al., 2017). We found that FSNs fire longer than PNs and earlier during licking, but not forelimb movements. PNs displayed more specific activity during movement performed with different effectors (i.e. licking and arm retraction), while most FSNs increased their discharge irrespective of the movement type. Computational analyses revealed that FSNs carried a greater amount of redundant information prior to PNs activation. Finally, optogenetic silencing of FSNs reduced spontaneous licking movement, suggesting that a global rise of inhibition contributes to the initiation and execution of spontaneous motor actions.

92

93 Materials and Methods

94 Experimental design and subject details

All experiments were carried out in accordance with the EU Council Directive 2010/63/EU and the 95 italian decree 26/2014 on the protection of animals used for scientific purposes, and were 96 approved by the Italian Ministry of Health (Authorization number 753/2015-PR). Animals were 97 98 housed in rooms at 22 °C with a standard 12h light/dark cycle. Food (standard diet, 4RF25 GLP Certificate, Mucedola) and water were available ad libitum, except for the experimental period, 99 during which mice were water-deprived overnight. Electrophysiological recordings were 100 101 conducted on 13 subjects. Experiments were carried out on 3-5 months old wild-type (C57BL6/J) 102 male mice. Six B6.Cg-Tg (Thy1-COP4/EYFP)18Gfng (ChR2) male mice expressing channelrhodopsin-2 (ChR2) mainly in corticofugal, layer V neurons were used to map 103 mouth/tongue movements in the ALM. For optotagging of FSNs, 2 PV-Cre male mice (Tanahira 104 105 et al., 2009) (B6;129P2-Pvalb tm1 (cre)Arbr/J, Jackson Laboratories, USA) were injected with an 106 excitatory ChR2-expressing AAV vector (see details below). Finally, for inhibition of FSNs during licking activity, 4 PV-Cre mice were injected with a modified inhibitory ChR2-expressing AAV 107 vector (see details below). 108

109 Surgery procedure and animal preparation

Viral injections. PV-Cre mice were deeply anesthetized with an intraperitoneal injection of avertin (0.020 ml/g) and positioned on a stereotaxic frame; cranial sutures were exposed and 112 used as reference. A small craniotomy was performed on the right ALM (1.8 mm lateral and 2.5 mm anterior to Bregma). For optotagging the FSNs, we injected 600 nl of the AAV9/2 vector 113 (pssAAV-2-hEF1α-dlox-hChR2(H134R) mCherry(rev)-dlox-WPRE-hGHp(A), ETH Zurich Viral 114 Vector Facility, 5.4×10¹² vg/ml) containing the double floxed ChR2 fused to an mCherry reporter, 115 116 thus expressed selectively in parvalbumin interneurons through Cre-mediated recombination (Spalletti et al., 2017; Tantillo et al., 2020), henceforth referred to as PV+ FSNs . For PV+ FSNs 117 optogenetic inhibition experiments, we injected 600 nl of the AAV1 vector (pAAV hSyn1-SIO-118 stGtACR2-FusionRed, 105677-AAV1, Addgene, 1.8×10¹³ vg/ml) containing the double floxed 119 120 modified soma-targeted anion-conducting ChR2 fused to FusionRed, allowing its selective 121 expression in PV+ FSNs. Viral vectors were injected using a microinjector (Nanoliter 2020 Injector, WPI), with an infusion rate of 90 nl/min at a 750 µm depth from the cortical surface. Skin 122 123 was sutured and animals allowed to awaken. Three weeks later, injected mice underwent surgical procedure for electrophysiological or behavioral experiment. 124

Surgical preparation for electrophysiological and behavioral experiments. Mice were deeply anesthetized and positioned on a stereotaxic frame; the scalp was partially removed, the skull cleaned and dried. A custom-made lightweight head post, was placed on the skull on the left hemisphere, aligned with the sagittal suture and cemented in place with a dental adhesive system (Super-Bond C&B). A thin layer of the dental cement was used to cover the entire exposed skull. For electrophysiological recordings, a ground screw was implanted above the cerebellum.

For acute recordings, a recording chamber was built using dental cement (resin adhesive cement, Ivoclar Vivadent) and centered on the right ALM (1.8 mm lateral and 2.5 mm anterior to Bregma, Fig. 1A). The skull over the recording area was covered by sterile low melting agarose Type III (A6138, Sigma-Aldrich, Inc.) and sealed with Kwik-Cast (WPI). On the day before the first acute recording session, 6 B6.Cg-Tg (Thy1-COP4/EYFP)18Gfng (ChR2) mice were anesthetized with ketamine (100 mg/kg) and xylazine (10 mg/kg) cocktail, the chamber cover removed and cortex was optogenetically stimulated following a grid with nodes spaced 500 µm. For each site, 139 optogenetic stimulation (3 ms single pulses, 0.2 Hz) was delivered by means of PlexBright Optogenetic Stimulation System (PlexonInc, USA) with a PlexBright LD-1 Single Channel LED 140 Driver (PlexonInc, USA) and a 473 nm Table-top LED Module connected to a 200 µm Core 0.39 141 NA optic fiber (ThorlabsInc, USA). Movements of tongue/mouth were collected by a second 142 143 experimenter, blinded to the stimulation coordinates. A small craniotomy (diameter, 0.5 mm) was 144 then performed over sites where the larger tongue/mouth movements could be evoked. In wild-145 type mice, the craniotomy was performed in the same region of Thy1-ChR2 mice. Finally, the chamber was filled with agarose and sealed. 146

For chronic implants, a squared craniotomy (side: 0.8 mm) was made over the right ALM (1.8 mm 147 148 lateral and 2.5 mm anterior to Bregma), partially covering the Rostral Forelimb Area (RFA, 1.2 149 mm lateral and 2 mm anterior to bregma, Fig. 1A). A planar multi shank 4x4 array (16 parallel microwires recording from their tips, Microprobes for Life Science) was positioned over the 150 craniotomy and microwires were inserted into the cortex, up to ~1000 µm depth to ensure better 151 stability of the signal. Then, the craniotomy was covered with low melting agarose and the array 152 fixed and embedded with dental cement (Super-Bond C&B and Paladur). Mice were allowed to 153 154 awaken and then housed separately.

155 Behavioral tasks and electrophysiological recordings

After recovering from surgery, mice were water restricted in their home cages, with food still available. Condensed milk was provided as a reward during the tasks and mice were also provided with water *ad libitum* for about 1 hour/day, following each recording session.

During the shaping phase, mice were placed in a U-shaped restrainer (3 cm inner diameter), head-fixed through the metal post cemented on their skull and habituated to lick reward drops, randomly provided by the experimenter through a feeding needle with no sensory cues enabling the animal to anticipate the delivery of the drop, which could be detected only by sniffing. Spontaneous licks were detected using a home-made piezoelectric licksensor implemented using Arduino. It has been set to precisely detect each time that the mouse tongue touches the spout, directly mounted on a piezoelectric sensor. We quantified the time between the first mouth opening and the first licksensor activation for each licking bout in 3 videos (120 fps) acquired during the recording sessions in 3 different animals. The licksensor did not alter neural trace with any artifact. Digital signals from the licksensor provided information about the licking movements directly to the recording apparatus.

170 Each shaping session lasted from 15 min up to 60 min for at least 3 consecutive days. Licking events were classified as either single or multiple licks. The start lick was defined as a movement 171 that was not preceded (for at least 0.6 s) by any other licking event. A single lick was a start lick 172 not followed by any other lick for at least 0.6 s; multiple licks were defined as start licks followed 173 by at least two other consecutive licks (≤ 0.4 s among consecutive licks). Time intervals lasting 174 for ≥ 1 s and distant at least 0.5 s from the end or the start of licking trials were considered as 175 resting intervals and used as a baseline for the analysis of neural activity. To assess if motivation 176 of mice could influence the proportion of single and multiple licks, the frequency distributions of 177 single and multiple licks were considered in our sessions. To normalize for different durations 178 179 among sessions, each recording session was divided in 10 time windows and the number of single and multiple licks in each window has been counted; the relative frequency of single and 180 181 multiple licks as a function of time along the session has been reported.

For identification of PV neurons in PV-cre mice, the site of AAV injection was illuminated with an optic fiber (200µm Core 0.39 NA, Thorlabs, USA). Optogenetic stimulation (50 0.2 s pulses, 0.2 Hz) was delivered by means of PlexBright System (Plexon, USA) with a PlexBright LD-1 Single Channel LED Driver (Plexon, USA) and a 473 nm Table-top LED Module. After spike sorting, PVpositive (i.e. FS) neurons were defined as neurons increasing their firing rate by 5 ms from the beginning of the blue light pulse (i.e. ChR2-positive neurons) and with a sustained activity for the entire stimulation length.

For the chronic recordings, in which forelimb-driven response was also assessed, head-fixed mice were shaped on a robotic platform, the M-Platform (Spalletti et al., 2014). Briefly, the M-Platform is composed of a linear actuator, a 6-axis load cell, a precision linear slide with an adjustable friction system and a custom-designed handle that is fastened to the left wrist of the 193 mouse. The handle is screwed onto the load cell, which permits a complete transfer of the forces applied by the animal to the sensor during each session. The session starts when the linear 194 actuator moves the handle forward and extends the mouse left forelimb by 10 mm (full upper 195 extremity extension). During recording sessions, the forepaw, contralateral to the implanted 196 197 ALM/RFA, is maintained in a slightly isometric extended position; however, the animal voluntarily tries to pull the handle back to stay in a more comfortable posture, by retracting its forelimb 198 199 (without any associated reward), and the force peaks exerted to attempt retractions are detected by the load-cell and offline aligned with neural signals. 200

In experiments with optogenetic inhibition of PV+ FSNs, 2 days post head-fixation implantation, 201 202 mice were head-fixed and habituated to receive the liquid reward, delivered automatically, 203 through an automatic peristaltic pump, 2 s after a 0.3 s acoustic-cue (4000 Hz). The pump was active for 0.3 s to deliver a drop of reward. After 2 days of habituation, a fiber optic was placed on 204 their injected (right) ALM and the cue-signaled reward was randomly delivered in presence or 205 absence of optogenetic stimulation. In a first set of mice (n = 2), the optogenetic stimulation 206 consisted of a 1 s blue light train (3 ms pulses intermingled by 3 ms interpulse intervals, 473 nm), 207 208 starting 1 s before the start of pump activation. In a second set of mice (n = 2), optogenetic stimulation was delivered 0.5 s before the start of pump activation. During the experiment, licking 209 activity was detected through the licksensor and the frequency of licks was measured in a time 210 window ranging from 0.5 s after start of reward delivery to 2.5 s later. 211

212 Immunohistochemistry

Mice were perfused transcardially with PBS followed by 4% PFA. Brains were post-fixed overnight and transferred to 30% sucrose PB solution before sectioning on a freezing microtome (Leica). 50-µm thick coronal free-floating sections were processed using standard fluorescent immunohistochemical techniques: as primary antibodies we used: NeuN (1:1000, Millipore), GFAP (1:500, Dako), Parvalbumin (1: 300, Synaptic System); as secondary antibodies we used: anti-guinea pig AlxaFluor 488 (1:500, Jackson Laboratories), anti-rabbit RRX (1:400, Jackson Laboratories). MCherry and FusionRed signals were not amplified with immunostaining.
 Micrographs have been acquired using a fluorescence microscope (Zeiss, Germany).

221 Single-unit recording and spike sorting

The electrophysiological data were continuously sampled at 40 kHz and bandpass filtered (300 Hz to 6 kHz), using a 16-channel Omniplex recording system (Plexon, Dallas, TX).

For acute recordings, a NeuroNexus Technologies 16-channel linear silicon probe with a singleshank (A1x16-3mm-50-177, 50 µm spacing among contacts) was slowly lowered into the ALM; the tip of the probe was placed at about 1000 µm depth using a fine micromanipulator (IVM, Scientifica). The recording chamber was filled with sterile saline solution (NaCl 0.9%). Before the beginning of the recording, the electrode was allowed to settle for about 10 min. For each animal, a number of one up to seven extracellular recording sessions were performed.

For chronic recordings, mice were recorded on up to 10-15 recording daily sessions per animal
over a 15 days period.

The extracellular recording data were processed to isolate spike events by a spike sorting software (Offline Sorter[™] v3.3.5, Plexon), using principal component analysis; events (spikedetection interval > 1.0 ms) that exceeded a 4 SDs threshold above the background were sorted. The spike waveforms were aligned at global minimum and the artifact waveforms were removed. The single-unit clusters were manually defined.

237 Data analysis

The recorded units were classified based on their average waveforms into putative pyramidal neurons (PNs) and putative fast-spiking neurons (FSNs). Two waveform parameters were used for the classification: the ratio between the height of the maximum peak and the initial negative trough, and the trough-peak time. A k-means clustering was applied. The clustering was verified by optogenetic tagging of PV-positive neurons.

The relation between single neuron activity and the events of the behavioral task was analysed
 using MATLAB (MathWorks). Peristimulus Time Histograms (PSTHs) were built aligning spike

245 events on the start lick, for both single and multiple licks, and on the onset of the force during forelimb pulling. Only intervals with stable unit activity were included and spikes were averaged 246 over 0.05 s with 0.01 s steps. The PSTH covered a time window of 1 s, from 0.6 s before the 247 starting event (lick or force onset) and 0.4 s after it. Responsive neurons were identified by 248 249 comparing firing activity in the PSTHs with the mean firing rate and an upper and lower threshold, calculated during resting periods (lasting \geq 1 s, and distant from event trials \geq 0.5 s). 250 251 Bootstrapping was used to estimate the thresholds; lower and upper thresholds were, respectively, the 2.5 and 97.5 percentile of the probability distribution function obtained during the 252 resting intervals. A unit was considered responsive for the licking behaviour or forelimb retraction 253 when, for at least three consecutive bins (0.03 s), its firing rate went over (enhanced neurons) or 254 under (suppressed neurons) the considered thresholds. 255

The onset of activity was defined as the first bin of the \ge 3 consecutive bins above/below the upper/lower threshold; the time of the bin in which the firing rate (spk/s) was maximum/minimum was considered as the peak time. To assess the influence of basal firing rate at rest (defined as above) on onset latency, a linear correlation was performed. To the same purpose, we pooled together FSNs and PNs with a licking-related activity and ordered them according to their resting firing rate (blinding the category they belong to); then, we compared the onset latency for each interquartile of FSNs and PNs.

The duration of the response was the number of bins above/below the upper/lower threshold. The intensity of activation was defined as:

265

area above/below the upper/lower threshold duration of the response

266

Licking-related firing rate heat maps report normalized spiking activity of FSNs and PNs with enhanced licking-related activity. Firing rate has been normalized as follows: threshold firing rate (red) was set to zero, firing rate above threshold was normalized on the maximum and firing rate below the threshold was normalized on the minimum firing rate of each neuron, obtaining spiking activity ranging from -1 to 1. Spatial selectivity for licking/forelimb activity was evaluated mapping the proportion of forelimb-,
licking- and licking/forelimb-related neurons among electrode positions of chronic arrays.
Specifically, we considered total number of neurons modulated by licking L (i.e. "L+" + "L-"),
forelimb F (i.e. "F+" + "F-") and licking/forelimb LF (i.e. "L+/F+" + "L+/F-" + "L-/F+" + "L-/F-").

276 Information content

We measured the information content (Shannon, 1948) in all neurons with significant lickingrelated modulation (facilitated or suppressed). We considered the mean firing rate of each neuron about two different sets of conditions. Set 1: 0.8 s intervals centered at single licks (see above) vs rest, i.e. randomly selected 0.8 s intervals during which animals were at rest, distant at least 1.5 s from other licking or rest intervals. Set 2: 0.8 s intervals centered at the onset of multiple licks (see above) vs rest.

The mean firing rate (mfr) associated with each trial was measured over the whole window. The mutual information of summed firing rates (E, mfr) between mfr and each set of events E was computed as follows:

Information of Summed FR (E, mfr) =
$$\sum_{e} P(e) \sum_{mfr} P(mfr \mid e) * log2(\frac{P(mfr \mid e)}{P(mfr)})$$

286 Where P (e) was the probability of the presentation of the specific event e, P (mfr) the probability 287 over all trials and all conditions of the neuron to have the mean firing rate mfr in a given interval, P (mfr | e) the probability of the mean firing rate mfr to be associated to the event e. Mean firing 288 289 rates were binned in N equipopulated bins, where N was the minimum value between the square 290 root of the total number of trials and the number of unique values in the array of mean firing rates. 291 To reduce the bias in the estimation of the information due to the limited dataset, a quadratic 292 extrapolation method was used (Panzeri et al., 2007). A statistically significant threshold was 293 obtained bootstrapping 100 times (shuffling the conditions associated to each trial), and, for a major solidity, only neurons with an IC > 95 percentiles of the bootstrapped distribution, in at least 294 295 one of the two combinations, were included, generating a subset of informative neurons.

We also calculated the information content over time: we considered 0.8 s before and 0.4 s after the first licking event, and we computed a local mean firing rate (Lmfr) over a moving average of 50 ms with 10 ms steps. Then, for each step we repeated the procedure described above. For this analysis we only used the subset of informative neurons described above.

For each recording session, we computed animal-wise the amount of information carried by summed firing rates of the recorded FSNs and PNs population. Each recording session has a different number of neurons and a different ratio between FSNs and PNs, for this reason, to be able to compare results from different recording sessions, the information of summed firing rates was computed considering N couples of neurons belonging to the same class for each recording. N was the minimum value between all the possible combinations of same-class-neurons and 40.

For each couple of neurons, information of summed firing rates was calculated with the followingequation:

Information of Summed FR (E, mfr 1,2)

$$= \sum_{e} P(e) \sum_{mfr \ 1,2} P(mfr \ 1,2 | e) * log2 \left(\frac{P(mfr \ 1,2 | e)}{P(mfr \ 1,2)}\right)$$

Where Information of Summed FR (E, ISF 1,2) is the information given by the summed firing rates of neuron 1 and 2, P (e) was the probability of the presentation of the specific event e, P (mfr 1,2) the probability that the sum firing rate of the neurons to have the mean firing rate mfr 1,2 over all trials of all conditions, P (mfr 1,2 | e) is the probability of the mean firing rate (mfr 1,2) to occur during the event e.

We used the same bias correction method and the same statistically significant threshold of the previous analysis. Only couples with an information of summed FR > 95 percentiles of the bootstrapped distribution, in at least one of the two combinations, were considered.

We then normalized the Information of Summed FR (E, ISF 1,2) generating the information of summed FR index to the sum of the information contained in the mean firing rate of neuron 1 and 2 calculated separately with the following equation: Information of Summed FR Index(1,2) = $1 - (\frac{ISFR(E, ISFR1,2)}{I(E, mfr1) + I(E, mfr2)})$

319 Where Information of Summed FR Index (1,2) is the normalized information carried by the sum of 320 the firing rate of neuron 1 and 2, ISFR (E, ISFR 1,2) and I (E, mfr1) are defined above.

When Information of Summed FR Index (1,2) is equal to 0 it suggests that the information carried by the means of the two neurons are mostly independent, while higher values suggest that the information is more dependent.

324 Statistical Analysis

All data are expressed as mean \pm standard error of the mean (SEM). Statistical tests were performed using Graphpad Prism 8.0 or SigmaPlot 12.0. Statistical significance was assessed using Wilcoxon Test, Mann-Whitney Test, One Way ANOVA, Paired t-test and Chi-square Test, as appropriate. Cumulative distributions were tested using Kolmogorov-Smirnov (K-S) twosample Test. All statistical analyses were performed on raw data. The level of significance was set at *p < 0.05, **p < 0.01, ***p < 0.001.

331

332 Results

333 Electrophysiological identification of FSNs and PNs in head-fixed behaving mice

To clarify the causal role of FSNs in initiation and execution of spontaneous movements, we performed extracellular recordings within the premotor areas associated with licking and forelimb pulling movements, namely the ALM and RFA, respectively (Fig. 1A). We functionally identified the ALM by verifying, with optogenetic mapping in 6 Thy1-ChR2 mice, that its stimulation evoked mouth/tongue movements, whereas the identification of RFA was made based on previous literature (Alia et al., 2016, Spalletti et al., 2017, Svoboda and Li, 2018).

We extracellularly recorded neuronal activity from 1452 units with either an acutely inserted single shank, 16-channels silicon probe (n = 10 mice, n = 693 units) or a chronic 16microelectrodes array (n = 3 mice; n = 759 units) from the ALM (and also RFA, during chronic recordings). Spike detection and sorting were performed offline (Barthó et al., 2004; Mitchell et
al., 2007; Niell and Stryker, 2010) to separate broad- and narrow-spiking neurons, classified as
PNs and FSNs, respectively (Fig. 1B, C).

To further validate the identification of FSNs, we performed extracellular recordings with 346 347 optogenetic stimulation in mice expressing ChR2 selectively in Parvalbumin-positive, fast-spiking 348 cells (Tantillo et al., 2020, Fig. 1D, E). FSNs waveforms were included in the dataset prior to 349 PNs/FSNs clustering: notably, all the optogenetically-tagged PV+ FSNs displayed a small trough to peak time and peak-trough ratio, coherently with their functional identification as putative 350 interneurons, thereby confirming the reliability of our identification method. Moreover, narrow-351 spiking movement-related neurons displayed higher baseline activity (Fig. 1F) and shorter inter-352 spike interval (ISI, Fig. 1G) than broad-spiking neurons, consistent with the classification of the 353 former as putative FSNs and of the latter as putative PNs. 354

355

356 Activity of PNs and FSNs in the ALM during licking

Water-restricted, head-fixed mice were allowed to lick drops of liquid reward spontaneously (not 357 358 signaled by any cue), available through a drinking spout, centered in front of the animal and 359 detecting licking events through a piezo-based licksensor (Fig. 2A). To guantify the latency between the onset of the licking movement and the licksensor activation, we analyzed 120 fps 360 361 videos of a subset (n = 3) of the recorded sessions (in different animals) and measured the 362 number of frames interposed between mouth opening onset and licksensor switching. We found 363 a latency of 61.9 ± 20.8 ms (mean ± SD, Fig. 2B). Offline, we categorized licking bouts based on their lick numerosity. We found bouts composed of up to 8 consecutive licking events (categories 364 including from 6 to 8 events were less represented, Fig. 2C). To assess if neural activity reflects 365 the sequential encoding of each motor chunk in a licking bout or if it is associated with the whole 366 sequence of movements, we analyzed isolated "single" (1 lick) and "multiple" (≥ 3consecutive 367 licks) bouts (see Methods). Due to the spontaneous nature of our task, we checked the time 368

distribution of single and multiple licks over the recording sessions to control motivation effects on licking behavior. We found a simultaneous gradual dispersion over time, consistent with the increasing satiation of animals, but importantly, we did not find differences in the distribution of single and multiple licks along the session (not significant Group x Time interaction, Fig. 2D)

373 Peristimulus time histograms (PSTHs) were created by aligning the spiking activity of each neuron to the first tongue touch of each licking bout (see example neurons in Fig. 2E). For each 374 neuron, the mean firing rate was compared with a threshold (Fig. 2F and Methods) to identify 375 significantly responsive neurons. Overall, in both acute and chronic recordings, we found 624 out 376 of 1452 units (36%) significantly modulated during movement, whereas the remaining were not 377 378 significantly modulated during motor activity. Out of 624 movement-related neurons, 251 (203 379 putative PNs, 48 putative FSNs, Table 1) were recorded in the first set of experiments with acutely inserted silicon probes in the ALM. The majority of putative PNs showed enhanced firing 380 rate during licking, and only 15% of them exhibited a suppressed discharge during licking epochs 381 (Fig. 2G). Among FSNs, the proportion of licking-suppressed neurons was lower (about 6%; Fig. 382 2H). 383

Both PNs and FSNs showed the maximum response modulation at the licking bout initiation, 384 385 even in the case of multiple licks, suggesting that their activity could contribute to the entire sequence rather than the generation of each individual lick. This can be clearly appreciated by 386 building mean PSTHs for the two classes of neurons (Fig. 3A, B). We found that in multiple licks, 387 by aligning neuronal spiking on the first lick of a bout, the PSTH displayed a unique peak before 388 the beginning of the series (Fig. 3B, average of all PNs and FSNs) while only a small fraction of 389 the recorded units (2% of FSNs and 5% of PNs, Fig. 3C, D) showed a series of recurrent peaks 390 time locked with each licking event. Consistently, comparing mean PSTHs aligned on the first or 391 392 the second lick in the series, both onset of the response (Fig. 3E) and peak of activity timing (Fig. 3F) were shifted backward of about 0.150 s relative to the alignment on the first lick, which 393 394 corresponds to the typical time lag between subsequent licking events in a series. These data support the hypothesis that neuronal discharge of both PNs and FSNs in the ALM is mainly 395

396 related to start the execution of the entire licking bout rather than the execution of individual licks397 in a series.

398 Next, we assessed the possible difference between PNs and FSNs in the encoding of licking 399 bouts made of single or multiple licks, starting from the evidence that individual neurons can 400 discharge differently prior and during these types of behavior (see neuron examples in Figure 2E). We plotted the percentages of PNs and FSNs modulated exclusively during single licks, 401 multiple licks, or both (Fig. 3G). The comparison reveals that the majority of both FSNs and PNs 402 discharge for licking bouts regardless of the number of lick events constituting the bout (either 1 403 or more than 2 licks), and that this behavior is prevalent among FSNs relative to PNs. These data 404 405 indicate that although single and multiple licks can be encoded differently, FSNs have a broader tuning than PNs. 406

407 FSNs show earlier and more sustained activation than PNs during licking

408 We next investigated PNs and FSNs firing activity during single and multiple licks (see Fig. 4A-D). 409 First, we analyzed the onset of the (enhanced or suppressed) response, revealing that most of 410 the recorded neurons exhibit a significant modulation prior to movement onset, independently from the forthcoming licking strategy (Fig. 4E), but onset of PNs discharge occurred earlier in 411 relation to multiple than single licks, whereas FSNs fired ~ 0.1 s earlier than PNs but with no 412 413 significant difference between multiple and single licks. A cumulative distribution curve of the onset for individual neurons (Fig. 4F, G) clearly indicate an earlier recruitment of FSNs. This early 414 activation of FSNs was not a by-product of their overall higher firing rate with respect to PNs, 415 since there was no correlation between resting firing rate and onset latency in licking-responsive 416 neurons (rho = -0.065, p = 0.197, Fig. 4H). Moreover, we did not find any effect of baseline firing 417 418 rate in explaining differences between PNs and FSNs onset, since comparison of onset latency 419 between PNs and FSNs with similar firing rate (same interguartile), showed an effect for the neuronal type but neither for the firing rate class, nor for the interaction (Fig. 4I). 420

Then, we examined the timing of the peak of activity (or suppression) for each neuron. In multiple licks, the average peak time was delayed for both PNs and FSNs (Fig. 5A. Cumulative distributions of the peak latency are reported in Figure 5B, C. A robust statistical difference between PNs and FSNs was present for multiple licks: specifically, one third of PNs reached their maximum firing rate before the onset of the licking bout, whereas about half of FSNs had their peak of activity prior to licking onset (Fig. 5C). Next, we explored the duration of neuronal response, which was greater for both PNs and FSNs when mice performed multiple vs single licks (Fig. 5D). Interestingly, the response duration was overall longer in FSNs during both single and multiple licks as compared to PNs (Fig. 5E, F).

Similar results were obtained by analyzing the magnitude of the activation of the two neuronal 430 classes. During multiple licks, both PNs and FSNs showed greater discharge than during a single 431 432 lick (Fig. 5G). It is worth noting that, as reported above (Fig. 2D), although we confirmed that 433 motivation has an effect on the total number of lick events over time, no difference between the rate of single vs multiple licks was observed, allowing us to safely exclude a role of satiation state 434 of the animals in causing the electrophysiological differences between single and multiple licks. 435 Furthermore, the FSNs displayed a higher activity relative to PNs, which was more evident in 436 multiple than in single licks (Fig. 5H, I). 437

Altogether, these findings show that FSNs have an earlier and sustained firing activity with respect to PNs during the movement, independently of the licking strategy – i.e. single or multiple licks - which nevertheless are coded by differential response patterns of both PNs and FSNs in terms of onset, peak discharge, duration and magnitude of their firing activity.

442 Information content of firing rate

We next computed, for all the previously identified responsive neurons, the mutual information between the firing rate and the behavioral states (i.e., rest, single lick and multiple licks; see Methods). The fraction of informative neurons was 0.74 for FSNs and 0.63 for PNs. Within the subset of informative neurons, FSNs carried vastly more information than PNs about the onset of both single (0.130 bits, FSNs; 0.074 bits, PNs) and multiple licks (0.221 bits, FSNs; 0.140 bits, PNs). 449 Coherently with an earlier onset of the response, FSNs information content ramped up earlier than that of PNs (Fig. 6A, B). Information carried by FSNs became 3 SD larger than baseline for 450 at least two consecutive bins ~0.05 s earlier than PNs. Comparing single licks and rest, the 451 information exceeded the threshold 0.25 s before lick detection in FSNs and 0.2 s in PNs. The 452 453 peak of information was reached at the tongue touch in FSNs and 0.03 s later in PNs. Multiple licks vs rest yielded similar results: the information exceeded the threshold 0.33 s before the first 454 licking event in FSNs and 0.27 s in PNs; the peak was reached 0.02 s after the event in FSNs 455 and 0.05 s in PNs. Temporal dynamics of the information content was similar to the FSNs and 456 PNs features shown by the results in previous section (Fig. 5) and global PSTHs (compare Fig. 457 6A, B with Fig. 3A, B). 458

We then computed the animal-wise amount of information carried by the summed firing rate of the recorded FSNs and PNs population and found that FSNs carried more redundant information. The Information of summed firing rate index (see Methods) is significantly higher for FSNs than for PNs (mean 0.26 for FSNs; 0.08 for PNs, single licks vs rest; mean 0.25 for FSNs; 0.20 for PNs, multiple licks vs rest; Fig. 6C).

464 Overall, these results suggest that the local firing rate of FSNs conveys a considerable amount of 465 information prior to PNs activation, further supporting the idea that a robust and coherent 466 inhibitory activity might be important before and during the movement.

467 Layer-specific responses of PNs and FSNs

468 Linear probes allowed us to investigate the laminar distribution of recorded neurons. Specifically, 469 units were classified as superficial (channels 1-8, \sim < 600 µm depth) or deep (channels 9-16, \sim > 470 600 µm depth). In our sample, about 25% of PNs and FSNs were recorded from superficial 471 layers. Figure 7A and 7B report the onset of activity for each recorded unit as a function of depth (i.e. channel number). While the average response onset of FSNs precedes the one of PNs 472 473 (consistently with Fig. 4E-G), a small proportion of PNs (especially in deep layers) appear to increase their firing rate earlier, simultaneously with FSNs. Furthermore, firing activity appears to 474 475 start earlier in deep relative to superficial layers (Fig. 7A, B, red-shaded part of panels).

Considering onset latency separately in deep or superficial PNs and FSNs, we substantially confirmed findings obtained over all cortical layers. In fact, FSNs activity starts significantly earlier than PNs activity in both superficial (Fig. 7C) and deep (Fig. 7D) layers during single licks. During multiple licks, the activity of FSNs starts significantly earlier than that of PNs in deep (Fig. 7F), but not in superficial (Fig. 7E) layers.

These results suggest that initial activity mostly begins in deep layers of ALM (Chen et al., 2017),
and involves both FSNs and PNs.

483 Direct comparison of the neuronal responses of PNs and FSNs during two motor acts

484 Early and sustained inhibition by FSNs during licking may be a general mechanism that contributes to action selection prior to movement onset, regardless of the effector to be used for 485 acting. To test this hypothesis, we compared the activity of a set of FSNs and PNs, recorded in 486 487 head-fixed mice during two types of motor tasks, i.e. a forelimb retraction task in addition to the licking task. We took advantage of a robotic platform (M-Platform, Allegra Mascaro et al., 2019; 488 489 Spalletti et al., 2017), which allows mice to perform several trials of spontaneous forelimb pulling 490 (without associated rewards), resulting in force peaks, recorded by a load cell embedded in the M-Platform (see Fig. 2A). Distribution of maximum force and duration of force peaks in our 491 dataset were reported in Fig. 8A and 8B. Neurons' discharge was aligned to the onset of force 492 493 peaks (Pasquini et al., 2018; Spalletti et al., 2014) (Fig. 8C). Animals were also allowed to perform spontaneous licking within the same experimental session, albeit in different epochs. In 494 the following sections, we describe the neuronal discharges during pulling and multiple licking 495 events (i.e. spaced by more than 0.6 s from any type of movement). 496

For these experiments we employed a planar 4x4 chronic array, centered on the ALM but exceeding the boundary with the adjacent RFA (Alia et al., 2016; Tennant et al., 2011, Fig. 1A, 9A). To allow greater stability during the recordings, electrode contacts were positioned in deep layers. We isolated n = 373 units (PNs, n = 313; FSNs, n = 60; mice, n = 3, Table 1), which were responsive to licking, pulling, or both. 502 We found a great proportion of neurons whose discharge was suppressed during licking, higher with respect to previous data collected in acute recordings. Specifically, 37% of PNs, whose 503 discharge was modulated during licking behavior showed movement-related suppression of their 504 discharge; a similar proportion (40%) of PNs responsive for forelimb retraction were also 505 506 suppressed. For FSNs, the percentages of suppressed neurons were similar (39.1%) for forelimb retraction, and lower (20.3%) for licking. These data suggest that pyramidal neurons as well as 507 508 FSNs located in deep layers are particularly susceptible to movement-related suppression. 509 Therefore, we analyzed enhanced and suppressed neurons separately (Table 2).

510 Lower motor selectivity for licking and forelimb movement in FSNs than PNs

511 Neuronal selectivity for each type of movement (i.e. multiple licks vs pulling) was assessed comparing distribution of FSNs and PNs whose activity was modulated selectively during multiple 512 licks (L), forelimb pulling (F), or both (LF). In particular, we subdivided the recorded units into 513 514 different functional classes, according to the movement-induced modulation of their discharge. Specifically, neurons responsive to only one type of movement were classified as 515 enhanced/suppressed by licking (L+, L-) or forelimb pulling (F+, F-). Neurons responsive to both 516 movements showed either a mutual (L+/F+, L-/F-) or opposite modulation (L+/F-, L-/F+) during 517 518 each motor task. We found that PNs (violet bars in Fig. 9B) were distributed across all functional classes. In contrast, the vast majority of FSNs (>72%) were mutually modulated (i.e., suppressed 519 or enhanced) by the two different movements (i.e., L+/F+, 50% and L-/F-, 20%) showing a 520 broader tuning than PNs (Fig. 9B), similarly to the data previously reported for "single" and 521 522 "multiple" licks (Fig. 3G). However, licking was the preferred neuronal response for all recorded 523 units, and even considering those neurons activated by both movements, the average peak firing rate (Fig. 9C) and the intensity of activation (Fig. 9D) were significantly lower during forelimb than 524 525 during licking activity both in FSNs and PNs, consistently with the anatomical location of the implanted array. To assess if PNs and FSNs licking/forelimb preference was related to the 526 527 location inside ALM, we compared the proportion of all forelimb-related neurons among electrode positions, over the region covered by the 4x4 chronic microelectrode array in the implanted mice 528

(see Methods). Overall, we found no evidence for a clear segregation of function at the level of single neurons in the ALM and the portion of sampled RFA, neither for PNs nor for FSNs (One way ANOVA: PNs, $F_{(15, 23)} = 0.97$, p = 0.51; FSNs, $F_{(11, 5)} = 1.26$, p = 0.42) (Fig. 9E, F).

We next compared the response onset and duration among the different populations of neurons. Consistently with results in acute recordings, concerning licking activity (Fig. 10A) enhanced FSNs started to discharge before facilitated PNs. Instead, during forelimb pulling a significant earlier activation of FSNs was not confirmed (Fig. 10B) since, as in laminar recordings (Fig. 7), a subset of pyramidal neurons (approx. 15%) modulated their discharges very early. Interestingly, the suppressed FSNs showed a delayed discharge onset relative to the enhanced FSNs, especially during licking (Fig. 10A, B).

In terms of duration of the response, this was significantly greater for the FSNs, specifically those excited during movement, considering both licking (Fig. 10C) and pulling (Fig. 10D). The suppressed FSNs showed a shorter duration of modulation, although not statistically different from that of enhanced FSNs (Fig. 10C, D). There was no difference in the discharge duration between enhanced and suppressed PNs (Fig. 10C, D).

The peak time was not modulated in enhanced FSNs compared to enhanced PNs during both licking (Fig. 10E) and forelimb retraction (Fig. 10F) while a general trend of a greater intensity of activation was found in enhanced FSNs with respect to PNs during both types of movements (Fig. 10G, H).

Altogether, these data support the previous laminar recordings in indicating an early and prolonged discharge of FSNs activated by licking, but not pulling, suggesting a specificity of the early inhibitory tone for the primary body effector associated to the considered area. Interestingly, the suppressed FSNs were modulated at longer latencies during movement generation.

552 Causal role of FSNs activation in movement facilitation

To assess a causal role of FSNs activity in licking movements we inhibited PV+ FSNs expressing anion-conducting ChR2 in the right ALM of PV-Cre mice (Fig 11A). In a first set of mice (n = 2), trials with 1 s of optogenetic silencing of FSNs prior to reward delivery were pseudorandomly administered together with an equal number of trials with no stimulation (Fig. 11B). In a second set of mice (n = 2) the 1 s optogenetic inhibition was started 0.5 s prior to reward delivery onset (Fig. 11C). We found that licking activity, monitored through the lick sensor after reward delivery, was significantly reduced in both cases during optogenetic inhibition (Fig. 11D, E, blue traces) compared to control trials (Fig. 11D, E, black traces). These data suggest that inhibitory neurons in the mouth region have a causal role in facilitating spontaneous licking movement.

562

563 Discussion

In the present study we demonstrated that FSNs in the mouth/face motor field of the mice 564 anterolateral premotor cortex fire in anticipation of PNs with a specific pattern of activation during 565 spontaneous licking, but not during forelimb movements. FSNs become active earlier, longer, and 566 more intensely than PNs, and also carry more information about movement onset than PNs. 567 568 Furthermore, this rise of inhibitory activity appears to causally contribute to the initiation and 569 execution of actions, as suggested by the results of our optogenetic silencing experiments. These findings are in agreement with a previous electrophysiological study examining the discharge of 570 FSNs and PNs in mouse primary motor cortex during sensory-triggered as well as voluntary 571 572 forelimb reaching movements (Estebanez et al., 2017), and support a role of early inhibition mediated by FSNs during motor activity by both primary motor and premotor areas. 573

Preparatory/ramping activity in ALM PNs has been shown to be maintained by a recurrent 574 575 excitatory loop that involves both the cortex and the ipsilateral thalamus (Guo et al., 2017). Since FSNs are directly reached by thalamic afferents (Lourenço et al., 2020b), this recurrent 576 thalamocortical loop may sustain persistent firing activity observed in FSNs. It is worth noting 577 that, although PNs were recruited later than FSNs during movement initiation in our study, a 578 579 fraction of PNs located in deep layers, was early-modulated. Despite the sampling bias of laminar recordings, which clearly favors the sampling of deep relative to superficial neurons and hence 580 581 suggest cautiousness in interpreting these findings, we reported a generally earlier involvement 582 of deeper neurons during licking behaviors. In particular, early-modulated deep PNs may represent preparatory "master" neurons that subsequently command downstream, more 583 executive PNs and FSNs. In keeping with our results, which concerns spontaneous behaviour, it 584 has been shown that preparatory activity appears first in deep layers of ALM during a task with an 585 586 instructed, delayed motor response (Chen et al., 2017). Concerning FSNs suppressed during movement execution, the onset data clearly show that they are consistently delayed with respect 587 to the other populations. Since PV+FSNs form a highly interconnected set of neurons (Lourenço 588 et al., 2020a), it is likely that the suppressed fast-spiking population receives direct synaptic input 589 from enhanced FSNs. 590

591 A general finding that applies to all types of recorded neurons is that the great majority of them do 592 not fire in relation to individual licking movements, nor are influenced by the number of licking movements in a bout (i.e. multiple vs single licks). Nonetheless, FSNs were less selective for the 593 movement type than PNs, which in turn exhibited a richer variety of behaviors, from enhanced to 594 suppressed discharge depending on the specific movement in relation to which they fired (i.e. 595 licking vs pulling). In contrast, the percentage of suppressed FSNs was lower, and they often 596 597 increased their firing rate during both pulling and licking movement, thus showing lower motor specificity. Accordingly, FSNs appear to carry more redundant information than PNs, consistently 598 599 with the fact that FSNs are known to be synchronized by electrical and chemical synapses (Lourenço et al., 2020b). In fact, previous studies showed that in the prefrontal cortex of mice 600 performing a sensory discrimination task, PV+FSNs were activated by all movement-related 601 602 events (sensory cues, motor action, and trial outcomes), while responses of PNs were diverse 603 and more selective (Pinto and Dan, 2015). The broader tuning of FSNs is also consistent with previous findings in sensory cortices - where interneurons were poorly selective for stimulus 604 features such as orientation (Hofer et al., 2011; Kerlin et al., 2010) - and in monkey parieto-605 606 premotor cortices - as shown by recent evidence concerning visual and motor tuning for object type during visually-guided grasping actions (Ferroni et al., 2021). 607

23

608 An additional important finding is that we couldn't identify a clear tuning map for the two investigated movements (licking and forelimb retraction), which involve two distinct effectors, 609 neither when PNs nor when FSNs were considered. From a comparative point of view, these 610 results are consistent with the findings in the monkey ventral premotor cortex, in which forelimb 611 612 and face/mouth representations largely overlap both in terms of functional properties and 613 electrically-evoked motor responses (Maranesi et al., 2012). Coherently, intracortical 614 microstimulation (ICMS) of the frontal cortex in mice showed a highly variable distribution of sites leading to forelimb/head movements in individual animals (Tennant et al., 2011), suggesting that 615 anatomical overlapping between the cortical representation of functionally-related effectors is an 616 evolutionarily conserved solution for motor control. 617

618 It has been hypothesized that the activity of interneurons, including FSNs, provides an inhibitory gate that prevents preparatory activity from causing undesired movements. If this were the case, 619 interneuron firing rates should be reduced around the time of movement, which was not observed 620 in the present experiments. Another possibility is that FSN-mediated inhibition may serve to 621 suppress other actions (e.g., movement of other body parts). If FSNs act to prevent adjacent 622 623 cortical modules from producing other movements, one would predict the existence of distinct licking- and forelimb-related FSNs which reciprocally inhibit the respective PNs. However, our 624 data do not provide support for such a model, as more than 50% of FSNs increase their 625 discharge during both licking and forelimb retraction. Thus, a sustained, overall rise in FSNs 626 activity appears to be required, likely to reach a critical level of inhibition for properly releasing 627 628 and maintaining motor activity. To probe this hypothesis, we employed optogenetic silencing of 629 FSNs activity prior and during reward delivery, demonstrating that in both cases there was a significant reduction in the frequency of spontaneous licking behavior during the time period 630 following the stimulation, supporting the idea that FSNs activity play a role in the initiation and 631 632 maintenance of sequential motor actions.

633 Despite the increase of inhibitory activity is known to be a general phenomenon linked to 634 movement execution, anticipation of FSNs activity across all cortical layers appears to be specific 635 for the motor action primarily represented in the investigated motor field. In fact, we focused our study on the ALM, which is an area primarily involved in the control of licking and mouth-related 636 actions: coherently, we observed a prevalence of neurons (both PNs and FSNs) responding to 637 licking rather than forelimb actions, and virtually no FSNs selectively activated during forelimb 638 639 movements. While in our study on a mouth/face premotor region we found early FSNs activity 640 during licking but not during forelimb retraction, early FSNs activation has been reported during forelimb movements when recordings were carried out in the forelimb motor cortex (Estebanez et 641 al., 2017), supporting a specific role of FSNs in shaping and sculpting the motor output primarily 642 influenced by a given cortical sector, likely acting on the response selectivity of nearby PNs. 643

In the motor cortex, the magnitude of inhibition directly affects tuning of individual PNs before and during movement execution both in mice (Galiñanes et al., 2018) and nonhuman primates (Georgopoulos et al., 1982; Merchant et al., 2008). Furthermore, the activity of FSNs might provide an inhibitory constraint that maintains firing rates of PNs within an "optimal subspace" (Afshar et al., 2011) that allows accurate movement (Churchland, 2006). Future studies should address these alternative hypotheses on the mechanistic role of FSNs in contributing to specification and initiation of voluntary movements.

In conclusion, our study contributes to clarifying the causal role of FSNs in driving, with a global rise of inhibition, the initiation and execution of specific, spontaneous motor actions by mouse premotor cortex.

654

655 References

- Afshar, A., Santhanam, G., Yu, B.M., Ryu, S.I., Sahani, M., Shenoy, K.V., 2011. Single-Trial
 Neural Correlates of Arm Movement Preparation. Neuron 71, 555–564.
 https://doi.org/10.1016/j.neuron.2011.05.047
- Alia, C., Spalletti, C., Lai, S., Panarese, A., Micera, S., Caleo, M., 2016. Reducing GABAA mediated inhibition improves forelimb motor function after focal cortical stroke in mice. Sci
 Rep 6, 37823. https://doi.org/10.1038/srep37823
- Allegra Mascaro, A.L., Conti, E., Lai, S., Di Giovanna, A.P., Spalletti, C., Alia, C., Panarese, A., 662 663 Scaglione, A., Sacconi, L., Micera, S., Caleo, M., Pavone, F.S., 2019. Combined Rehabilitation Promotes the Recovery of Structural and Functional Features of Healthy 664 Neuronal Networks 3474-3485.e6. 665 after Stroke. Cell Reports 28. https://doi.org/10.1016/j.celrep.2019.08.062 666
- Barthó, P., Hirase, H., Monconduit, L., Zugaro, M., Harris, K.D., Buzsáki, G., 2004.
 Characterization of neocortical principal cells and interneurons by network interactions and
 extracellular features. J Neurophysiol 92, 600–608. https://doi.org/10.1152/jn.01170.2003
- Chen, T.-W., Li, N., Daie, K., Svoboda, K., 2017. A Map of Anticipatory Activity in Mouse Motor
 Cortex. Neuron 94, 866-879.e4. https://doi.org/10.1016/j.neuron.2017.05.005
- Churchland, M.M., 2006. Neural Variability in Premotor Cortex Provides a Signature of Motor
 Preparation. Journal of Neuroscience 26, 3697–3712.
 https://doi.org/10.1523/JNEUROSCI.3762-05.2006
- Churchland, M.M., Shenoy, K.V., 2007. Temporal Complexity and Heterogeneity of SingleNeuron Activity in Premotor and Motor Cortex. Journal of Neurophysiology 97, 4235–4257.
 https://doi.org/10.1152/jn.00095.2007

Estebanez, L., Hoffmann, D., Voigt, B.C., Poulet, J.F.A., 2017. Parvalbumin-Expressing
GABAergic Neurons in Primary Motor Cortex Signal Reaching. Cell Reports 20, 308–318.
https://doi.org/10.1016/j.celrep.2017.06.044

Ferroni, C.G., Albertini, D., Lanzilotto, M., Livi, A., Maranesi, M., Bonini, L., 2021. Local and system mechanisms for action execution and observation in parietal and premotor cortices. Curr Biol S0960-9822(21)00547–9. https://doi.org/10.1016/j.cub.2021.04.034

Galiñanes, G.L., Bonardi, C., Huber, D., 2018. Directional Reaching for Water as a Cortex Dependent Behavioral Framework for Mice. Cell Rep 22, 2767–2783.
 https://doi.org/10.1016/j.celrep.2018.02.042

Gao, Z., Davis, C., Thomas, A.M., Economo, M.N., Abrego, A.M., Svoboda, K., De Zeeuw, C.I., Li, N., 2018. A cortico-cerebellar loop for motor planning. Nature 563, 113–116. https://doi.org/10.1038/s41586-018-0633-x

- Georgopoulos, A., Kalaska, J., Caminiti, R., Massey, J., 1982. On the relations between the
 direction of two-dimensional arm movements and cell discharge in primate motor cortex. J.
 Neurosci. 2, 1527–1537. https://doi.org/10.1523/JNEUROSCI.02-11-01527.1982
- Godschalk, M., Lemon, R.N., Kuypers, H.G.J.M., Van Der Steen, J., 1985. The involvement of
 monkey premotor cortex neurones in preparation of visually cued arm movements.
 Behavioural Brain Research 18, 143–157. https://doi.org/10.1016/0166-4328(85)90070-1
- Guo, Z.V., Inagaki, H.K., Daie, K., Druckmann, S., Gerfen, C.R., Svoboda, K., 2017. Maintenance
 of persistent activity in a frontal thalamocortical loop. Nature 545, 181–186.
 https://doi.org/10.1038/nature22324
- Guo, Z.V., Li, N., Huber, D., Ophir, E., Gutnisky, D., Ting, J.T., Feng, G., Svoboda, K., 2014. Flow
 of cortical activity underlying a tactile decision in mice. Neuron 81, 179–194.
 https://doi.org/10.1016/j.neuron.2013.10.020

702 Hocherman, S., Wise, S.P., 1991. Effects of hand movement path on motor cortical activity in awake, behaving rhesus monkeys. Exp Brain Res 83. https://doi.org/10.1007/BF00231153 703 Hofer, S.B., Ko, H., Pichler, B., Vogelstein, J., Ros, H., Zeng, H., Lein, E., Lesica, N.A., Mrsic-704 Flogel, T.D., 2011. Differential connectivity and response dynamics of excitatory and 705 inhibitory Neurosci 14, 1045-1052. 706 neurons in visual cortex. Nat 707 https://doi.org/10.1038/nn.2876

Isaacson, J.S., Scanziani, M., 2011. How inhibition shapes cortical activity. Neuron 72, 231–243.
 https://doi.org/10.1016/j.neuron.2011.09.027

Isomura, Y., Harukuni, R., Takekawa, T., Aizawa, H., Fukai, T., 2009. Microcircuitry coordination
 of cortical motor information in self-initiation of voluntary movements. Nat Neurosci 12,
 1586–1593. https://doi.org/10.1038/nn.2431

Kaufman, M.T., Churchland, M.M., Shenoy, K.V., 2013. The roles of monkey M1 neuron classes
in movement preparation and execution. Journal of Neurophysiology 110, 817–825.
https://doi.org/10.1152/jn.00892.2011

Kerlin, A.M., Andermann, M.L., Berezovskii, V.K., Reid, R.C., 2010. Broadly Tuned Response
Properties of Diverse Inhibitory Neuron Subtypes in Mouse Visual Cortex. Neuron 67, 858–
871. https://doi.org/10.1016/j.neuron.2010.08.002

Komiyama, T., Sato, T.R., O'Connor, D.H., Zhang, Y.-X., Huber, D., Hooks, B.M., Gabitto, M.,
 Svoboda, K., 2010. Learning-related fine-scale specificity imaged in motor cortex circuits of
 behaving mice. Nature 464, 1182–1186. https://doi.org/10.1038/nature08897

Li, N., Daie, K., Svoboda, K., Druckmann, S., 2016. Robust neuronal dynamics in premotor cortex
 during motor planning. Nature 532, 459–464. https://doi.org/10.1038/nature17643

Liu, B., Li, Y., Ma, W., Pan, C., Zhang, L.I., Tao, H.W., 2011. Broad Inhibition Sharpens
 Orientation Selectivity by Expanding Input Dynamic Range in Mouse Simple Cells. Neuron
 71, 542–554. https://doi.org/10.1016/j.neuron.2011.06.017

Lourenço, J., De Stasi, A.M., Deleuze, C., Bigot, M., Pazienti, A., Aguirre, A., Giugliano, M.,
 Ostojic, S., Bacci, A., 2020a. Modulation of Coordinated Activity across Cortical Layers by
 Plasticity of Inhibitory Synapses. Cell Reports 30, 630-641.e5.
 https://doi.org/10.1016/j.celrep.2019.12.052

Lourenço, J., Koukouli, F., Bacci, A., 2020b. Synaptic inhibition in the neocortex: Orchestration
 and computation through canonical circuits and variations on the theme. Cortex 132, 258–
 280. https://doi.org/10.1016/j.cortex.2020.08.015

Maranesi, M., Rodà, F., Bonini, L., Rozzi, S., Ferrari, P.F., Fogassi, L., Coudé, G., 2012.
Anatomo-functional organization of the ventral primary motor and premotor cortex in the
macaque monkey: Organization of the ventral frontal motor cortex. European Journal of
Neuroscience 36, 3376–3387. https://doi.org/10.1111/j.1460-9568.2012.08252.x

Merchant, H., de Lafuente, V., Peña-Ortega, F., Larriva-Sahd, J., 2012. Functional impact of
 interneuronal inhibition in the cerebral cortex of behaving animals. Prog Neurobiol 99, 163–
 178. https://doi.org/10.1016/j.pneurobio.2012.08.005

Merchant, H., Naselaris, T., Georgopoulos, A.P., 2008. Dynamic Sculpting of Directional Tuning
 in the Primate Motor Cortex during Three-Dimensional Reaching. Journal of Neuroscience
 28, 9164–9172. https://doi.org/10.1523/JNEUROSCI.1898-08.2008

Messier, J., Kalaska, J.F., 2000. Covariation of Primate Dorsal Premotor Cell Activity With
 Direction and Amplitude During a Memorized-Delay Reaching Task. Journal of
 Neurophysiology 84, 152–165. https://doi.org/10.1152/jn.2000.84.1.152

Mitchell, J.F., Sundberg, K.A., Reynolds, J.H., 2007. Differential Attention-Dependent Response
 Modulation across Cell Classes in Macaque Visual Area V4. Neuron 55, 131–141.
 https://doi.org/10.1016/j.neuron.2007.06.018

Murakami, M., Vicente, M.I., Costa, G.M., Mainen, Z.F., 2014. Neural antecedents of self-initiated actions in secondary motor cortex. Nat Neurosci 17, 1574–1582. https://doi.org/10.1038/nn.3826

Niell, C.M., Stryker, M.P., 2010. Modulation of Visual Responses by Behavioral State in Mouse
 Visual Cortex. Neuron 65, 472–479. https://doi.org/10.1016/j.neuron.2010.01.033

Panzeri, S., Senatore, R., Montemurro, M.A., Petersen, R.S., 2007. Correcting for the Sampling
 Bias Problem in Spike Train Information Measures. Journal of Neurophysiology 98, 1064–
 1072. https://doi.org/10.1152/jn.00559.2007

Pasquini, M., Lai, S., Spalletti, C., Cracchiolo, M., Conti, S., Panarese, A., Caleo, M., Micera, S.,
 2018. A Robotic System for Adaptive Training and Function Assessment of Forelimb
 Retraction in Mice. IEEE Trans. Neural Syst. Rehabil. Eng. 26, 1803–1812.
 https://doi.org/10.1109/TNSRE.2018.2864279

Pi, H.-J., Hangya, B., Kvitsiani, D., Sanders, J.I., Huang, Z.J., Kepecs, A., 2013. Cortical
 interneurons that specialize in disinhibitory control. Nature 503, 521–524.
 https://doi.org/10.1038/nature12676

Pinto, L., Dan, Y., 2015. Cell-Type-Specific Activity in Prefrontal Cortex during Goal-Directed
 Behavior. Neuron 87, 437–450. https://doi.org/10.1016/j.neuron.2015.06.021

Polack, P.-O., Friedman, J., Golshani, P., 2013. Cellular mechanisms of brain state-dependent
gain modulation in visual cortex. Nat Neurosci 16, 1331–1339.
https://doi.org/10.1038/nn.3464

Poo, C., Isaacson, J.S., 2009. Odor representations in olfactory cortex: "sparse" coding, global
inhibition, and oscillations. Neuron 62, 850–861.
https://doi.org/10.1016/j.neuron.2009.05.022

Riehle, A., Requin, J., 1993. The predictive value for performance speed of preparatory changes in neuronal activity of the monkey motor and premotor cortex. Behavioural Brain Research 53, 35–49. https://doi.org/10.1016/S0166-4328(05)80264-5

- Sachidhanandam, S., Sermet, B.S., Petersen, C.C.H., 2016. Parvalbumin-Expressing GABAergic
 Neurons in Mouse Barrel Cortex Contribute to Gating a Goal-Directed Sensorimotor
 Transformation. Cell Rep 15, 700–706. https://doi.org/10.1016/j.celrep.2016.03.063
- Shannon, C.E., 1948. A Mathematical Theory of Communication. Bell System Technical Journal
 27, 379–423. https://doi.org/10.1002/j.1538-7305.1948.tb01338.x
- Spalletti, C., Alia, C., Lai, S., Panarese, A., Conti, S., Micera, S., Caleo, M., 2017. Combining
 robotic training and inactivation of the healthy hemisphere restores pre-stroke motor
 patterns in mice. Elife 6. https://doi.org/10.7554/eLife.28662
- Spalletti, C., Lai, S., Mainardi, M., Panarese, A., Ghionzoli, A., Alia, C., Gianfranceschi, L.,
 Chisari, C., Micera, S., Caleo, M., 2014. A robotic system for quantitative assessment and
 poststroke training of forelimb retraction in mice. Neurorehabil Neural Repair 28, 188–196.
 https://doi.org/10.1177/1545968313506520
- Svoboda, K., Li, N., 2018. Neural mechanisms of movement planning: motor cortex and beyond.
 Curr Opin Neurobiol 49, 33–41. https://doi.org/10.1016/j.conb.2017.10.023
- Swanson, O.K., Maffei, A., 2019. From Hiring to Firing: Activation of Inhibitory Neurons and Their
 Recruitment in Behavior. Front Mol Neurosci 12, 168.
 https://doi.org/10.3389/fnmol.2019.00168

Tan, A.Y.Y., Brown, B.D., Scholl, B., Mohanty, D., Priebe, N.J., 2011. Orientation Selectivity of
 Synaptic Input to Neurons in Mouse and Cat Primary Visual Cortex. Journal of
 Neuroscience 31, 12339–12350. https://doi.org/10.1523/JNEUROSCI.2039-11.2011

Tanahira, C., Higo, S., Watanabe, K., Tomioka, R., Ebihara, S., Kaneko, T., Tamamaki, N., 2009. Parvalbumin neurons in the forebrain as revealed by parvalbumin-Cre transgenic mice. Neurosci Res 63, 213–223. https://doi.org/10.1016/j.neures.2008.12.007

Tantillo, E., Vannini, E., Cerri, C., Spalletti, C., Colistra, A., Mazzanti, C.M., Costa, M., Caleo, M.,
 2020. Differential roles of pyramidal and fast-spiking, GABAergic neurons in the control of
 glioma cell proliferation. Neurobiology of Disease 141, 104942.
 https://doi.org/10.1016/j.nbd.2020.104942

- Tennant, K.A., Adkins, D.L., Donlan, N.A., Asay, A.L., Thomas, N., Kleim, J.A., Jones, T.A., 2011.
 The Organization of the Forelimb Representation of the C57BL/6 Mouse Motor Cortex as
 Defined by Intracortical Microstimulation and Cytoarchitecture. Cerebral Cortex 21, 865–
 876. https://doi.org/10.1093/cercor/bhq159
- Vallone, F., Lai, S., Spalletti, C., Panarese, A., Alia, C., Micera, S., Caleo, M., Di Garbo, A., 2016. 807 Post-Stroke Longitudinal Alterations of Inter-Hemispheric Correlation and Hemispheric 808 809 Dominance in Mouse Pre-Motor Cortex. PLoS ONE 11, e0146858. https://doi.org/10.1371/journal.pone.0146858 810

811 Weinrich, M., Wise, S.P., 1982. The premotor cortex of the monkey. J Neurosci 2, 1329–1345.

Wise, S.P., Mauritz, K.H., 1985. Set-related neuronal activity in the premotor cortex of rhesus
monkeys: effects of changes in motor set. Proc R Soc Lond B Biol Sci 223, 331–354.
https://doi.org/10.1098/rspb.1985.0005

815	Wu, G.K., Arbuckle, R., Liu, B., Tao, H.W., Zhang, L.I., 2008. Lateral Sharpening of Cortica
816	Frequency Tuning by Approximately Balanced Inhibition. Neuron 58, 132–143
817	https://doi.org/10.1016/j.neuron.2008.01.035

820 Figures Legends

Figure 1. Electrophysiological recordings and PNs vs FSNs identification A. A schematic 821 representation of the dorsal surface of the mouse brain showing the relative position of the 822 putative ALM (blue) and the putative RFA (green). Magnification on the right shows the recording 823 824 area (red square). The schematic diagram shows optogenetically identified movement 825 representations in ALM, in particular, tongue-responsive area (vellow), whiskers-responsive area (violet) and mouth-responsive area (orange). The red square represents the chronic microarray 826 827 position and the black dots indicate single microwires disposed in a 4x4 configuration. The blue 828 rectangle shows the acute recording area. B. Scatter plot of spike waveform parameters for all 829 recorded units (n = 1452). The violet and green filled squares represent individual putative PNs 830 (movement-related or not, violet and light violet, respectively) and FSNs (movement-related or not, green and light green, respectively), respectively. The orange filled triangles show spike 831 832 shapes of individual PV+ FSNs (activated at short latency by light). C. Average spike waveforms 833 for all units, PNs, FSNs and PV+ FSNs, aligned to minimum and normalized by trough depth. All waveforms are displayed in the inset (top). D. Representative ALM portion of a PV-Cre mouse 834 injected with the floxed ChR2-mCherry AAV (20x). MCherry reporter (red) indicates selective 835 836 expression in parvalbumin-positive (PV) neurons stained by immunohistochemistry (green). Scale bar, 100 µm. E. Representative raster plot and PSTH showing increased firing rate in response to 837 200 ms light pulses of an ALM ChR2+/PV+ FSNs recorded in a PV-Cre mouse injected with the 838 floxed ChR2-mCherry AAV. F, G. Mean firing rate (F) and maximum position of interspike 839 intervals (ISI, G) of PNs and FSNs. K-S Test, **p < 0.01. 840

841

Figure 2. FSNs and PNs are modulated during spontaneous licking in mice *A*. Schematic representation of a head-fixed mouse in the behavioral setup. In the bottom left, a scale bar of the licking behavior and a forelimb force peak (N) are represented as a function of time (s). *B*. Frequency distribution of latencies between licksensor activation (alignment event) and real onset of licking (first mouth movement detected in 120 fps videos). On average the movement onset 847 started 61.9 ± 20.8 ms (mean ± SD) before licksensor detection. C. Distribution of licking bouts based on the number of consecutive licks in a bout. Total number of licking events are reported 848 as a function of the number of licks in the series (composed by 1 to 8 licks). D. Average 849 distribution of single and multiple licks among sessions. Each recording session is divided in 10 850 851 time windows. The number of single and multiple licks in each time window is reported as the relative frequency of single and multiple licks for each session. Repeated Measures ANOVA, 852 Group, F = 25.60, p < 0.001, Time, F = 44.58, p < 0.001, Group x Time, F = 0.77, p = 0.64. Data 853 represented as mean ± shaded SEM. E. Seven examples of ALM neurons during licking task, in 854 single (left column) and multiple (right column) licks. Spike rasters and PSTHs are reported for 2 855 FSNs and 5 PNs in both single and multiple licks. Averaging window, 100 ms. Orange squares 856 represent licks (i.e. tongue touches) for each trial. F. Representative peristimulus time histogram. 857 858 The black line represents the average firing rate calculated during resting periods, black dotted lines the upper and lower threshold. The three black squares indicate the first, the maximum and 859 the last point over the threshold. The orange dotted lines and the orange arrows indicate the 860 861 onset of the activity and the peak time, respectively. The blue line shows the duration of the activity, representing the time over the threshold. The pink area is the area above the threshold. 862 The intensity of activation is defined as the pink area divided by duration of the activity. G, H. 863 864 Proportion of all responsive putative PNs - enhanced, violet, or suppressed, light violet - (G) and 865 putative FSNs – enhanced, green, or suppressed, light green – (H) during the licking activity. On the right, representative examples of raster plots and corresponding PSTHs showing enhanced 866 867 (left) and suppressed (right) neurons. The red dotted lines represent the upper thresholds, the green dotted lines the lower ones, the black line is the mean baseline firing rate. Time = 0 868 corresponds to the first lick, not preceded by other licks for at least 0.6 s. PNs suppressed vs 869 FSNs suppressed, Z-Test, z = 1.65, p = 0.09. 870

871

Figure 3. FSNs and PNs in ALM encode entire licking bout during single and multiple licks. *A*, *B*. Average PSTHs for all PNs (violet) and FSNs (green) in a 1 s window (0.6 s before and 0.4 s after the licking event) during single (A) and multiple (B) licks. Time 0 >(ertical red bars) 875 corresponds to the first lick. The second and the third bar in multiple licks indicate the mean position (± SEM, orange shades) of the second and the third lick, respectively. C, D. 876 Representative PSTHs of a PN (C) and a FSN (D) showing lick-by-lick modulation in a 1 s 877 window (0.6 s before and 0.4 s after the licking event) during multiple licks. Time 0 (vertical red 878 879 bars) corresponds to the first lick. The second and the third bar in multiple licks indicate the mean position (± SEM, orange shades) of the second and the third lick, respectively. E, F. Histograms 880 of the onset of the response (E) and the peak time (F) of PNs and FSNs obtained aligning PSTHs 881 to the first or the second lick of a licking bout. Wilcoxon Test, ***p < 0.001. G. Percentage of PNs 882 and FSNs responsive to both single and multiple licks, or selective for single or multiple licks. Chi-883 square Test, $\chi^{2}_{(1)}$ = 5.18, p = 0.023. 884

885

886

Figure 4. FSNs show earlier activation than PNs during licking in single and multiple licks A - D. 887 Heat maps for all positively modulated PNs (A, B) and FSNs (C, D) ordered by the onset of the 888 889 response, during both single and multiple licks. Normalized spiking activity is reported, ranging from -1 to 1. Threshold firing rate (red) was set to zero, firing rate above threshold is normalized 890 891 on the maximum and the one below threshold on the minimum for each neuron. E. Violin plots of 892 onset of the response, defined as the first latency above or below the thresholds on PSTHs, for 893 PNs (left) and FSNs (right), during single and multiple licks (always aligned to the first lick). Wilcoxon Test, *p < 0.05. F, G. Cumulative distribution of the onset of the response for all PNs 894 and FSNs during a single isolated lick (F) or multiple licks (G). The red shaded lines indicate the 895 confidence interval (61.9 ± 20.8 ms) of movement initiation, the first mouth movement before 896 licksensor activation. K-S Test, Single, p = 0.001, Multiple, p < 0.001. H. Correlation between 897 mean firing rate and onset latency in all recorded neurons. Rho = -0.0650, p = 0.197. I. All 898 899 neurons were pooled and then grouped in interquartile ranges, according to their resting firing rate. Latency of activation of FSNs and PNs was then compared for each interquartile. A Two-900 way ANOVA showed that factor neuronal type explained a large fraction of variance (F = 19.9, p 901 < 0.0001) while the factor interguartile did not (F = 2.18, p = 0.08). There was no interaction 902

between the factor interquartile and the factor neuronal type (F = 0.33, p = 0.8). Data are represented as mean \pm SEM.

905 Figure 5. FSNs show more sustained activation than PNs during licking. A. Violin plots of the peak time of PNs (left) and FSNs (right) during single and multiple licks (always aligned to the 906 907 first lick). The peak discharge is significantly delayed for both PNs and FSNs during multiple licks. Wilcoxon Test, p < 0.05, ***p < 0.001. **B**, **C**. Cumulative distribution of the peak time for all PNs 908 909 and FSNs during a single isolated lick (B) or consecutive multiple licks (C). The red shaded lines indicate the confidence interval (61.9 ± 20.8 ms) of movement initiation, the first mouth movement 910 before licksensor activation. K-S Test, Single, p = 0.064, Multiple, p = 0.0063. D. Violin plots of 911 912 the duration of the response of PNs (left) and FSNs (right), during single and multiple licks. 913 Wilcoxon Test, ***p < 0.001. E, F. Cumulative distribution of the duration of the response for all PNs and FSNs during a single isolated lick (E) and consecutive multiple licks (F). K-S Test, 914 Single, p = 0.0158, Multiple, p = 0.0269. G. Violin plots of the intensity of activity of PNs (left) and 915 FSNs (right), during single and multiple licks. Wilcoxon Test, PNs, **p < 0.01, ***p < 0.001. H, I. 916 Cumulative distribution of the intensity of activation for all PNs and FSNs during a single isolated 917 918 lick (H) and multiple licks (I). K-S Test, Single, p = 0.065, Multiple, p = 0.0051.

Figure 6. FSNs convey a considerable amount of information and prior to PNs activation. *A*, *B*. Information carried by firing rate of PNs (violet) and FSNs (green) about the presence of single (A) and multiple (B) licks. Information is computed over 0.05 s bins (with a sliding time window of 0.01 s width) in a 1 s window (0.6 s before and 0.4 s after the licking event). Lower and higher shades represent, respectively, the 25 and 75 percentile. Wilcoxon Test, p < 0.001. *C*. Information of summed firing rate index for couple of PNs and FSNs of the same recording session for both single and multiple licks. Mann-Whitney Test, *p < 0.05, **p < 0.01.

Figure 7. Relative temporal firing dynamics between FSNs and PNs is conserved over layers *A*, *B*. PNs (violet) and FSNs (green) depth distribution (across sixteen channels probe) of the onset
of the activity in a 1 s window (0.6 s before and 0.4 s after the licking event) during single (A) and
multiple (B) licks. *C*, *D*. Cumulative distribution of the onset of the response for superficial (C) and

deep (D) PNs and FSNs during a single isolated lick. K-S Test, Single - Superficial, *p = 0.0198. K-S Test, Single - Deep, **p = 0.0062. *E*, *F*. Cumulative distribution of the onset of the response for superficial (E) and deep (F) PNs and FSNs during multiple licks. K-S Test, Multiple -Superficial, p = 0.150. K-S Test, Multiple - Deep, **p = 0.0019.

934

Figure 8. ALM FSNs and PNs are modulated during spontaneous forelimb pulling A, B. 935 936 Frequency distribution of force peaks (A) and duration (B) of forelimb retraction. Averaging windows, 0.03 N (force peaks, A) and 500 ms (duration, B). C. Six examples of ALM and RFA 937 neurons, 3 FSNs and 3 PNs, are reported during licking task - in single (left column) and multiple 938 939 licks (central column) - and during forelimb retraction (right column). For each panel, in the top, spike rasters and PSTHs are reported for each neuron in all the three conditions; in the top right 940 941 of the figure, the force during forelimb retraction is reported. Averaging window, 100 ms. Orange 942 squares represent licks for each trial, green triangles the forelimb retraction for each trial.

943

944 Figure 9. FSNs exhibit lower selectivity than PNs for licking behavior and forelimb retraction. A. Representative image of 4 microwires traces after removal of implanted chronic electrodes (20x 945 tile, scale bar, 500 µm). The immunostaining against the neuronal marker (NeuN, green) and 946 947 reactive astrocytes (GFAP, red) show the site of microwires insertion (yellow lines) in a coronal 948 section of the ALM. B. Functional distribution of neurons responsive for licking (L), forelimb pulling (F) or both of them (LF), classified as enhanced (+) or suppressed (-) by the movement. 949 Chi-square test, $\chi^2_{(7)}$ = 20.19, p = 0.0052. *C*, *D*. Peak of activity and intensity of activation for all 950 PNs (violet) and FSNs (green) increasing their discharge during both forelimb retraction (F) and 951 multiple licks (L) tasks. Peak of activity, Paired t-test, PNs - Enh, $t_{(1, 91)} = 3.97$, ***p = 0.0001, 952 FSNs - Enh, $t_{(1, 30)}$ = 3.17, **p = 0.0035. Intensity of activation, Paired t-test, PNs - Enh, $t_{(1, 91)}$ = 953 4.47, ***p < 0.0001, FSNs - Enh, t_(1, 30) = 4.07, ***p = 0.0003. *E*, *F*. Proportion of PNs (E) and 954 FSNs (F) selective for forelimb pulling, multiple licking or both, among electrode positions over 955 956 the region covered by the 4x4 chronic microelectrode array in the ALM and the portion of sampled RFA. 957

distribution of the onset of the response for all neurons during a licking bout. The red shaded 960 lines indicate the confidence interval (61.9 ± 20.8 ms) of movement initiation, the first mouth 961 movement before licksensor activation. Enhanced neurons are represented as continuous lines 962 (PNs, violet; FSN, green); dotted lines indicate the suppressed PNs and FSNs. Enhanced PNs vs 963 suppressed PNs, K-S Test, #p = 0.043. Enhanced FSNs vs suppressed FSNs, K-S Test, §§p = 964 0.0090. Enhanced PNs vs enhanced FSNs, K-S Test, **p = 0.0069. B. Cumulative distribution of 965 the onset of the response (t = 0 corresponds to force peak beginning) for all neurons during the 966 forelimb retraction. Enhanced PNs vs suppressed PNs, K-S Test, p = 0.91. Enhanced FSNs vs 967 suppressed FSNs, K-S Test, p = 0.12. Enhanced PNs vs enhanced FSNs, K-S Test, p = 0.081. 968 969 C. Cumulative distribution of the duration of the response for all neurons during a licking bout. Enhanced FSNs vs suppressed FSNs, K-S Test, p = 0.610. Enhanced PNs vs suppressed PNs, 970 K-S Test, p = 0.987. Enhanced PNs vs enhanced FSNs, K-S Test, ***p = 0.0009. D. Cumulative 971 972 distribution of the duration of the response for all neurons during the forelimb retraction. Enhanced PNs vs suppressed PNs, K-S Test, p = 0.137. Enhanced FSNs vs suppressed FSNs, 973 K-S Test, p = 0.216. Enhanced PNs vs enhanced FSNs, K-S Test, *p = 0.029. E. Cumulative 974 975 distribution of the peak time for all neurons during a licking bout. Enhanced PNs vs enhanced FSNs, K-S Test, p = 0.0967. Red shaded lines, as in (A). F. Cumulative distribution of the peak 976 977 time for all neurons during the forelimb retraction. Enhanced PNs vs enhanced FSNs, K-S Test, p 978 = 0.283. G. Cumulative distribution of the intensity of activation for all neurons during a licking

Figure 10. FSNs show more sustained activation than PNs during forelimb pulling. A. Cumulative

bout. Enhanced PNs vs enhanced FSNs, K-S Test, p = 0.0665. *H.* Cumulative distribution of the
intensity of activation for all neurons during the forelimb retraction. Enhanced PNs vs enhanced
FSNs, K-S Test, p = 0.0789.

982

958

959

Figure 11. Optogenetic FSNs inhibition reduced licking behavior. *A*. Representative ALM
 micrograph (20x) of a PV-Cre mouse injected with the floxed AAV5-stGtACR1-FusionRed.

985 FusionRed reporter (red) shows specific expression of the floxed AAV in Parvalbumin-positive (PV) neurons (green), stained with immunohistochemistry. Scale bar, 100 µm. B, C. Schematic of 986 licking tasks with optogenetic silencing of FSNs in the right ALM for 1 s. The inhibition starts 1 s 987 (B) or 0.5 s (C) prior to the reward delivery onset and lasts until the liquid drop delivery or 0.5 s 988 989 later, respectively. D, E. Frequency distribution of licks during the licking task of 2 mice during the Light Off (black traces) and the Light On (blue traces) trials. The dotted black lines (0 s) indicate 990 the reward delivery. Blue shaded areas represent the ALM PV+ FSNs optogenetic inhibition 991 interval in Light On trials. Graphs on the right represent average licks for each session (n = 4-5) 992 993 of the 2 mice in a 2.5 s interval (gray shaded areas of the left graphs), during the light off and light 994 on trials. Top, Paired t-test, $t_{(1, 9)} = 2.30$, *p = 0.0468. Bottom, Paired t-test, $t_{(1, 7)} = 3.068$, *p = 0.018. 995

996

997 Tables

Table 1. Total number of recorded units during acute and chronic experiments. The modulated
PNs and FSNs are also reported.

	Total Recorded Units	Modulated Units	PNs	FSNs
Acute Exp	693	251	203	48
Chronic Exp	759	373	313	60

1000

1001

1002 **Table 2.** Number of neurons in different functional classes. Lick, licking; FP, forelimb pulling; Enh,

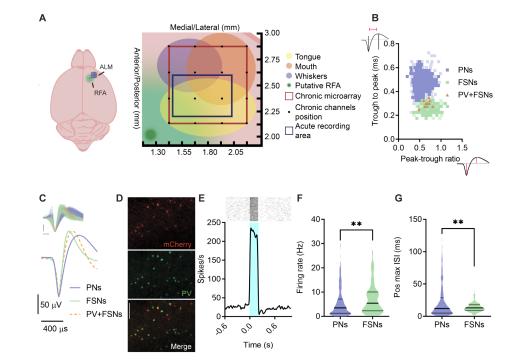
1003 enhanced; Supp, suppressed.

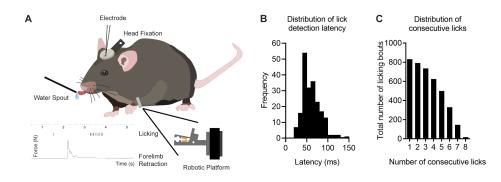
	Lick	Lick	Lick Enh / FP	Lick Enh /	Lick Supp /	Lick Supp /	FP	FP
	Enh	Supp	Supp	FP Enh	FP Supp	FP Enh	Supp	Enh
PNs	52	31	31	96	55	27	6	15
FSNs	7	2	9	31	11	-	-	-

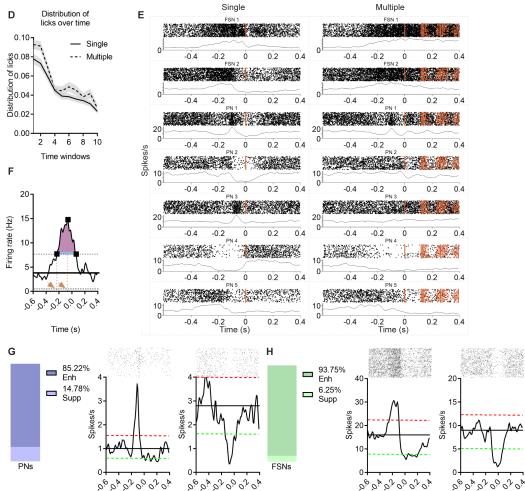
1004

1005

1006







Time (s)

Time (s)

Time (s)

JNeurosci Accepted Manuscript

